Bull. Chem. Soc. Ethiop. **2024**, 38(5), 1439-1452.
DOI: https://dx.doi.org/10.4314/bcse.v38i5.19

ISSN 1011-3924
Printed in Ethiopia
Online ISSN 1726-801X

MECHANICAL AND HEAT TRANSFER BEHAVIOUR OF ELECTRO-DEPOSITED NICKEL-ZIRCONIA COATING

J. K. Manoj[1], U. Arunachalam[2], M. Mathanbabu[3] and A. Kajavali[4]

[1]Department of Mechanical Engineering, Satyam College of Engineering and Technology, Kanyakumari Dist-629301, Tamilnadu, India
[2]Department of Mechanical Engineering, University College of Engineering Nagercoil, Kanyakumari Dist-629004, Tamilnadu, India
[3,4]Department of Mechanical Engineering, Government College of Engineering, Bargur, Krishnagiri-635104, Tamilnadu, India

(Received February 2, 2024; Revised June 16, 2024; Accepted June 18, 2024)

ABSTRACT. Thermal barrier coatings (TBCs) are often applied to base metals exposed to excessive temperatures to protect them from the harsh operating thermal cycle load conditions and to enhance their functionality. For this research, nickel and zirconia was coated over a mild steel substrate by electro-deposition or co-deposition method. While selecting appropriate electro-deposition parameters, this study analyses the convection and conduction heat transfer characteristics and mechanical behaviours of a nickel-zirconia co-deposit over a mild steel substrate. The better-quality deposition is formed with thicknesses of 10 µm and 50 µm. The microstructure and morphological analyses were conducted using scanning electron microscope (SEM). The phase analysis was conducted using X-ray diffraction analysis (XRD). The porosity, hardness and wear behaviours were measured as per the American Society for Testing and Materials (ASTM). The results showed that nickel-zirconia coating has better performance. The coating's convection and conduction heat transfer potential are investigated using a specially designed and constructed experimentation apparatus. Compared to an uncoated panel, heat transfer studies on nickel-zirconia coatings demonstrate that nano-coatings with a particle size of about 92 nm show a significant temperature drop with varied coating thicknesses and heat inputs for different heat inputs.

KEY WORDS: Thermal barrier coatings, Electro deposition, Conduction heat transfer, Convection heat transfer, Nickel-Zirconia

INTRODUCTION

Stainless steel has a wide range of commercial and technical uses. Because of its greater cost and corrosive nature, it must be protected from the working environment; hence, heat barrier coatings must be utilized to increase its performance and longevity [1, 2]. Engineering or functional coatings, namely thermal barrier coatings are extensively employed in industry to enhance the engineering component's surface performance [3]. The coating may be achieved by spraying two commercial alloys with differing compositions. When operating at excessive temperatures, the vast sections of aircraft components and rockets are exposed to tremendous temperatures and loads. A thorough investigation of the mechanical characteristics of various alloys may shed light on how to avoid failures in high-temperature applications [4]. It has been determined that in the future, thermal barrier coatings (TBCs) will need to be better suited to the thermal safety requirements expected over the next ten years. Therefore, it's crucial to understand how these coatings behave and fail under high temperatures and high thermal gradient cycling situations. This will help to design better TBCs [5]. There has been an increase in the use of novel materials for contemporary power production systems, such as gas turbines and more powerful, dependable engines that can meet the rising energy demands. Thermal barrier coatings have allowed gas turbines to operate at greater temperatures, increasing performance. Thermal insulation, corrosion, and high-temperature erosion prevention are provided by multilayer systems [6]. Ni-

*Corresponding authors. E-mail: manojscet20@gmail.com

ZrO_2 composite coatings are a kind of coating made up of nickel and zirconium oxide and are used in various applications. Nickel and zirconia are compatible because their thermal expansion coefficients and elastic moduli are similar.

Non-hardened particles are present in composite coatings, but their size and distribution within the coatings' matrix composition are also important factors in determining the hardness of the composite coating. A thermal barrier coating is required for the blades of a gas turbine to work effectively at high temperatures using a simulation study of the uncoated blade model. The researchers investigated the blade model with various coating contents. According to their findings, zirconium carbide is a ceramic material that is the best option for gas turbine blade coating due to its low density of 6.56 g/cc [7]. The oxidation behavior of electro-deposited nickel and Ni-ZrO_2 (9.9 vol%) was studied for 2–8 hours between 873 K and 1173 K using a thermogravimetric technique. The results demonstrate that the system followed a parabolic rate profile at 1073 K and 1173 K and a diffusion process controlled that oxidation. Ni-lower ZrO_2 oxidation rate constant demonstrated its resilience to high-temperature oxidation over electro-deposited nickel. [8]. At around 1170 °C, pure zirconia undergoes a phase shift from monoclinic to tetragonal, followed by a volume change and frequently results in fracture development in the coating. Stabilizers like yttria may prevent this. The most common TBC material is 6–8 wt.% yttria partly stabilized zirconia [9]. This research focuses on the advanced applications of nickel-zirconia coatings in various industries. The outcome of the research provided clarity on the use of nickel-zirconia coating for a specific application. Hence, this coating has a wide application for thermal protection on electronic gadgets in the missile cone during flight. The telecom communication system box is normally coated with this coating in satellite communications. It is a good wear-resistant coating applied to moving components in mechanical heat engines and machines. As it has improved wear characteristics, it replaces the hard chromium coating used in conventional automobile components. This coating replaces the hazardous chromium coating and protects the environment. Zirconia, when mixed with nickel to form a composite, has an improved hardness of nearly 980 Vickers, making it suitable for many engineering applications. Because of its composite nature, this coating also has improved corrosion resistance, making it useful in marine applications. Additionally, zirconia coating is employed in the nuclear sectors on corrosion-resistant/protection areas in power plants. Finally, by adopting the electroplating technique, one can control the thickness of coating manually and possess the ease of fabrication on steel. Nano nickel-zirconia composites may exhibit exceptional mechanical properties. Many experiments will be conducted in this area, potentially revealing numerous unexpected physio-mechanical properties. The greatest brinell hardness, impact strength, and compression strength were determined when ZrO_2 was reinforced at 6 wt.% due to the existence of a larger amount of hard ZrO_2 [10]. The microhardness of electroless nickel plated ZrO_2 Ni-NCZ is over 20% greater than that of Ni-ZrO_2. Ni-NCZ has higher microhardness and corrosion resistance than Ni-ZrO_2 due to the larger amounts of co-electrodeposited second phase particles, greater change in Ni microstructure, smaller Ni crystallite size, and stronger bonds between matrix and second phase particles [11]. Spray parameters of TBC, such as input power, spray distance, and powder feed rate, have significance in determining coating quality. Among the three factors, input power has the greatest influence on coating characteristics, followed by standoff distance and powder feed rate as key spray parameters. TBCs are widely applied in power plants, marine industry and aerospace industries [12, 13].

EXPERIMENTAL

Materials

A mild steel plate was taken as a cathode on which nickel-zirconia is to be deposited. A pure nickel rod (99.9% pure) was used as an anode in this process. Among the several electrolytic baths, sulphamate bath was preferred because of the low stress. Zirconia particles of 300 μm diameter were directly added in the electrolytic solution.

This study uses a nickel sulphamate solution for co-deposition of nickel-zirconia over a mild steel surface and to show the convective and conductive heat transfer characteristics of a co-deposited nickel-zirconia coating. Figure 1 shows the electroplating setup. The coating thickness, current density, and composition of the bath can be varied by varying the deposition time. The thermal transfer characteristics of two different film thicknesses of 10 µm and 50 µm were examined.

Figure 1. Electroplating setup for co-deposition.

Surface morphology

The surface morphology of the deposit exhibits numerous intriguing aspects related to the deposition mechanism. Furthermore, the surface topography has been observed to change with variations in pH, temperature, current, and agitation. The deposit's grain structure should be one of the four sorts of structures: columnar, fibrous, fine grain, forbidden, or very fine grains.

Larger grain size and three-dimensional growths are observed as the thickness of the nickel zirconia deposit increases. This might be owing to increased particle concentration and vertical development, as well as nano-sized particles in nature, as a reduction in grain size is noticed, and zirconia is dispersed uniformly throughout the deposit.

Nickel zirconia co-deposition

While supplying the direct current to the electrodes, oxidation occurs in nickel anode and nickel ions from anode get dissolved in sulphamate electrolyte to maintain the nickel ion concentration. Zirconia powder is directly added to the sulphamate bath. Alloys containing metals, such as molybdenum, tungsten, zirconium, germanium cannot be deposited alone. An induced co-deposition technique is involved to drag the zirconia particles along with nickel ions. The cations are attracted towards opposite charged electrodes. The ions which got deposited over the required surface by reduction lead to the formation of a thin layer of coating. Mechanical stirrer was employed at the speed of 600 rpm and used to produce turbulence mixing. Electrical heater was used to heat the electrolytic solution and maintained the temperature level at 55 ℃. Optimal conditions were analysed to achieve thicknesses of 10 µm and 50 µm, followed by coating on a mild steel surface. Figure 2 shows the architecture and as-coated specimens.

Experimental investigation

For the experimental examination, source blocks made of cast iron or aluminium were mounted over mild steel specimens with and without nickel-zirconia coatings. The tests were conducted using cast iron and aluminium blocks at various temperature ranges. The surface temperatures of the steel plate and coatings were measured using attached thermocouples. The energy input to the system was adjusted to achieve a maximum temperature of 300 °C for aluminium blocks and 600 °C for cast iron blocks. Coated surfaces with thicknesses of 10 µm and 50 µm were employed for the studies.

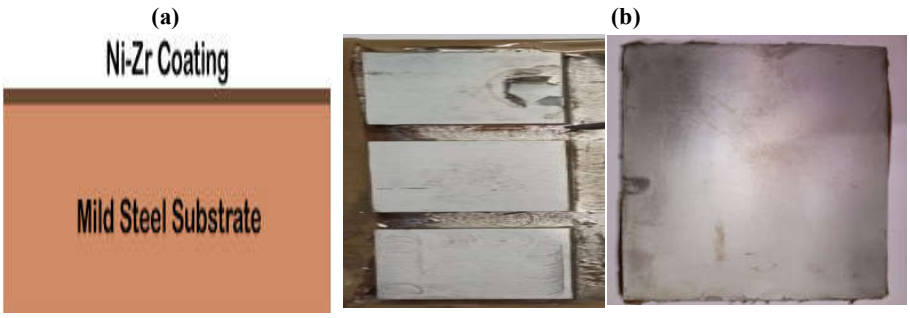

Figure 2. (a) Coating architecture and (b) as-coated specimens.

Electrical connections were meticulously verified before turning on the alternating current power supply to the variable transformer. The source block gets its energy supply from this variable transformer. The energy input to the source was steadily increased and maintained until a steady state was reached. The steady state was established once the temperature difference was 0.1 °C, which may take up to 90 min. The data acquisition system began continuously recording the temperature of the coating's surface at 15-second intervals as soon as the power was turned on. The surface temperatures of the coated and uncoated substrates were measured in three different locations using thermocouples. For calculations and analysis, the average value of temperatures in different locations is considered. The experiment was carried out using the same method with coatings that were 50 and 10 microns thick.

The experimental research analysed the characteristics of heat transfer by conduction of the electro-deposited nickel-zirconia coating over a surface of mild steel substrate and compared it with those of mild steel substrate without coating. To retain the heating element on all sides, two 90 mm x 45 mm x 30 mm slabs of aluminium or cast iron were utilised. To ensure that the heat conduction occurred only in the positive Y direction, high-grade insulating materials composed of an asbestos sheet were inserted between the bottom block and the heating source.

Heat flux is provided to the test specimen by the heater inserted between the blocks. The aforementioned intrinsic component was enclosed in a large, rectangular box-like enclosure, with the annular space between them filled with firmly packed glass wool. A nichrome wire was wrapped around a mica sheet to create the heating element. Perfect insulation is established around all surfaces of the source elements except the top surface by using very good insulation materials that provide air-tight contact between both vertical sides and the bottom base surface.

When achieving a steady state, there were no temperature inclines in the ‘x’ and ‘z’ directions, ensuring heat flow was one-dimensional. For this experiment, a one-dimensional equation of the Fourier law of heat conduction without the generation of heat was considered. The heater's power supply may be changed across an extensive range depending on the heat flux needs. On the surface of the uncoated and coated mild steel specimens, three sheathed K-type stainless thermocouples were placed. Dual plates of the same size as the substrate were used to direct the thermocouple lead so that the thermocouple sensing tip touches the appropriate spot on the substrate. The thermocouples were calibrated before fitting. The thermocouples and compensating wires were linked to a data acquisition system, which records the uncoated and coated specimen surface temperatures for different heat energy inputs. Using aluminium and cast-iron source blocks, the tests were carried out until the surface temperature successively reached 300 °C and 600 °C progressively from the ambient temperature. The heat loss at the surface in contact between the plate and the source material was eliminated. All trials were carried out under regulated and conventional conditions.

Mechanical and heat transfer behaviors

Wear properties

Wear is the damage to a solid surface caused due to relative motion between the surface and a contacting substance. Electro-deposited coatings are typically not effective for applications requiring wear resistance at temperatures above 500 to 600 °C. However, the use of composite coatings offer promise for higher temperature. Wear was produced by the sliding action of an abrading wheel rubbing the specimen inward and outward direction. The Taber Abraser is used as a lubricant and determines wear under dry conditions at room temperature. In the Taber Abrader Unit with a load of 1000 grams, weight loss for 1000 cycles was measured.

As per the ASTM (American Society for Testing and Materials) standards, in the Taber Abraser method for metallic coatings, weight loss per 1000 grams for 1000 rotations is directly represented as the wear index. With the reference of ASTM standard JIS H 8503, weight loss 0.056 per 1000 grams for 1000 rotation is measured as a wear index of nickel zirconia. Nickel zirconia deposit exhibits a very low wear index in room conditions. Low-wear index metals have an application in many industries, including the food industry and paper industry, and are widely used in cutting tools. Figure 3 shows the coated specimen after 1000 rotation and the wear index for various metals.

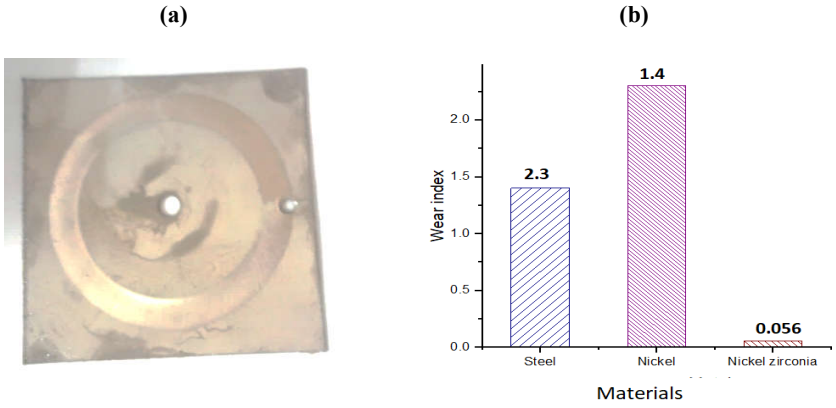

Figure 3. (a) Coated specimen after 1000 rotation and (b) wear index for various metals.

Hardness properties

For measuring the hardness of the coating, a 50 grams load is applied for 15 seconds on the nickel zirconia deposit. The micro-Vickers hardness HV (kg/mm^2) is used to calculate by the formula,

$V = 1845 \times (P/d^2)$

where d (mm) is the diagonal of the Vickers indentation and P (gm) is the applied load.

Nickel zirconia alloy electro-deposits produced by sulphamate bath exhibit microhardness value of 740-780VHN. Nickel Zirconia has a high micro hardness value of 740-780 VHN, which indicates that this may replace hard chromium in some cases. Figure 4 shows the hardness indentation image and Vickers hardness value for conventional metals.

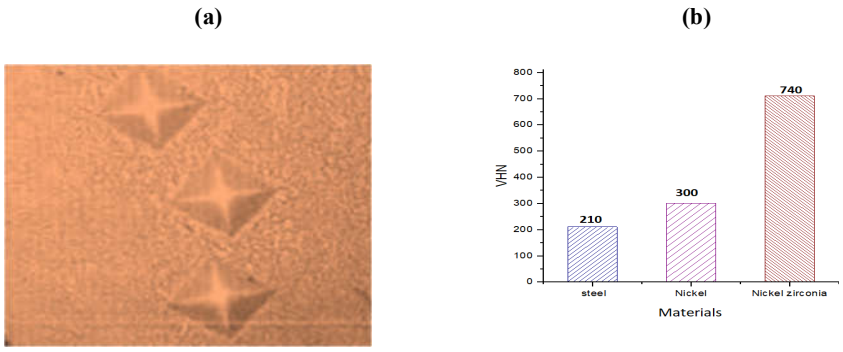

Figure 4. (a) Hardness indentation image and (b) Vickers hardness value for conventional metals.

The zirconia coatings are used in extreme conditions with high temperatures and a decreasing atmosphere. For instance, zirconia coating enables operating temperatures to exceed 1300 °C. The electro-deposition parameters examine the impact of bath temperature on nickel deposit grain size. Deviations of more than 5 ± °C from the optimal temperature may adversely affect coating quality, deposition rate, and other aspects. Surface characterization of Ni alloy composites is done using wear, roughness and microhardness.

Convective heat transfer behavior

The experimental setup for convection research includes the ability to represent the hot air at varied velocities and temperatures on the test workpiece in order to examine the convective behavior of the coated workpiece. The air is supplied through the 46 mm inner diameter pipe portion by an air blower, which is the major source of hot air. To control the flow of air through the pipe conduit, a non-return valve is installed in the route. The pipe surfaces through which the air flows are neatly covered by a heater wrapped around them. The heat of the air is determined by the energy provided to the heater. An orifice plate of 15 mm diameter is mounted at the intake of the pipe section to measure the velocity of air passing through this pipe. On the panel board, there is a U-tube water manometer attached to monitor the discharge of the flowing air. The pipe section's output is shaped into a funnel-like piece to expose the hot air over the workpiece. Two magnetic rods are used to keep the workpiece in place and expose it to the hot air. The tests were carried out for two different valve openings (VO1 and VO2) with different energy inputs.

To conduct the studies at different temperature ranges, two sets of valve openings with varied velocities and five distinct levels of energy inputs were used. The thermocouples were linked to record the temperatures of the coatings' and steel plate's surfaces. The experiments were carried out on coated surfaces with thicknesses of 10 µm and 50 µm. All tests were carried out under controlled conditions.

When the temperature difference was measured to be 0.1 °C after nearly 90 min, a steady state was achieved. The data logger constantly recorded the temperature of the coating's surface at 15-second intervals. Three thermocouples were used to determine the surface temperatures of the coated and uncoated surfaces, and the average value was used for computations and assessment. The same process was used to test coatings with thicknesses of 10 µm and 50 µm. The experiment was carried out for two distinct valve opening positions, VO1 and VO2. Figure 5 shows the location of temperature measurements in the air stream.

Estimation of velocity of the flowing air

The discharge and velocity of the flowing air for the different valve positions of VO1 and VO2 were determined as follows: h_w - difference in pressure head (m of H_2O), h_a - difference in pressure head (m of air), ρ_a - Density of flowing air (1.293 kg/m^3), ρ_w - Density of water (1000 kg/m^3), d_o - Diameter of an orifice (0.015 m), C_d - Co-efficient of discharge (0.62), D - Inside diameter of pipe section (0.046 m), A_f - Flow area of the pipe section (1.661×10^{-3} m^2), U - Velocity of air (m/s), Q - Discharge or volume flow rate of air (m^3/s).

$$h_a = \frac{\rho_w \times h_w}{\rho_a} \tag{1}$$

$$Q = C_d \ \frac{\pi}{4} d_0^2 \ \sqrt{2gh_a} \tag{2}$$

$$U = \frac{Q}{A_f} \tag{3}$$

Uncertainty analysis

The errors are calculated using the fewest counts and the sensitivity of the measurement devices employed in this study. The flow pattern of the fluids exposed to the coatings has the greatest influence on their convective heat transfer ability. Reynold's number defines the type of flow, which can be derived from the velocity of the fluid medium, the geometric parameters of the section, and the properties of the flowing fluids at bulk mean temperature. The uncertainty in Reynold's number is determined as follows:

$$Re = \frac{UD}{\nu} \tag{4}$$

where Re - Reynold's number, U - Velocity of the flowing fluid (m/s), D - Diameter of the pipe section (m), ν - Kinematic viscosity of the fluid (m^2/s).

$$Re = \frac{UD}{\nu}$$

$$\Delta Re = \left(\left(\frac{d(Re)(\Delta U)}{dU} \right)^2 + \left(\frac{d(Re)(\Delta D)}{dD} \right)^2 \right)^{1/2}$$

$$\frac{d(Re)}{dU} = \frac{D}{N} \quad \frac{d(Re)}{dD} = \frac{U}{\nu} \qquad \frac{\Delta(Re)}{Re} = \left(\left(\frac{\Delta U}{U} \right)^2 + \left(\frac{\Delta D}{D} \right)^2 \right)^{1/2}$$

Assuming a 2% variation in velocity and 1% variation in geometric dimensions,

$$\left[\left(\frac{\Delta U}{U} \right) = 2\% \right] \text{ and } \left[\left(\frac{\Delta D}{D} \right) = 1\% \right]$$

$$\frac{\Delta \mathrm{Re}}{\mathrm{Re}} = 0.02236$$

$$= 2.236\%$$

RESULTS AND DISCUSSION

VO 1 Condition (full opening)

In this VO1 opening condition of a foot valve, the discharge and velocity are 6.944×10^{-3} m^3/s and 4.18 m/s, respectively. Reynolds number of the flowing air ranges from 5518 to 7211, and hence the flow follows the turbulent behaviour. (The critical Reynolds number will be 2300 for the internal flow through the circular section). The variation in Reynold's number is due to the change in the temperature of the air. Effect of VO1 condition (full valve opening) with various responses is shown in Figure 5.

At 99.75 kW/m^2 heat input, the temperature of the uncoated panel was found to be 87.38°C, while the temperatures of 79.16 °C and 77.01 °C were observed on the 10 µm and50 µm coated panels, respectively. A nearly 9.41% reduction in temperature was calculated in a 10 µm coated panel, while an 11.87% reduction in temperature was noticed in a 50 µm coated panel. The energy input gradually enhanced to a value of 236.5 kW/m^2, the temperature of an uncoated surface plate was found to be 144.11 °C, while temperature indicator recorded a temperature of 127.08 °C on the 10 µm coated panel and 122.74 °C on 50 µm coated panel. Nearly 11.82% of the reduction in temperature was noticed in the 10 µm coated panel, and 14.83% of the reduction in temperature was observed in the 50 µm coated panel.

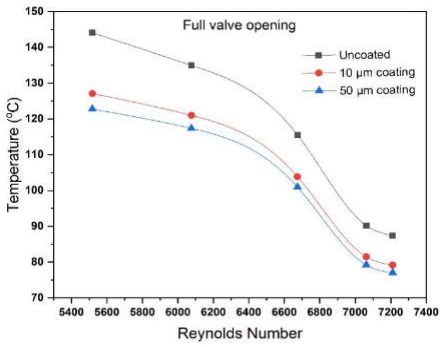

(a) Temperature variation with turbulence temperature.

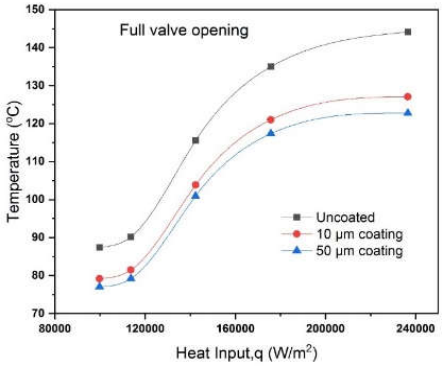

(b) Temperature - heat input.

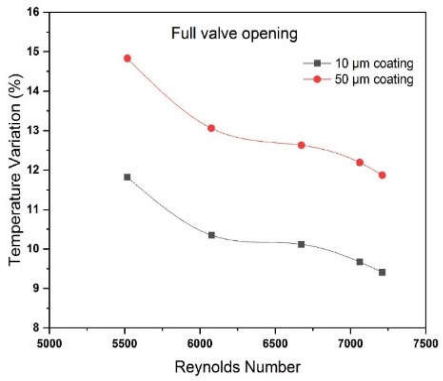

(c) Variation of temperature with Reynolds number.

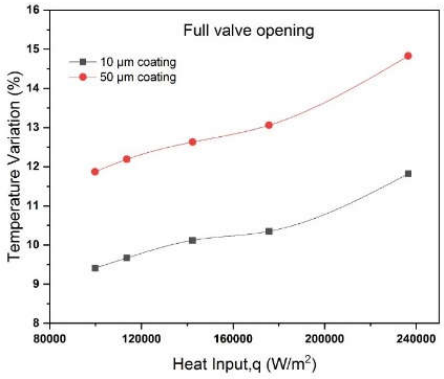

(d) Temperature variations of the coating.

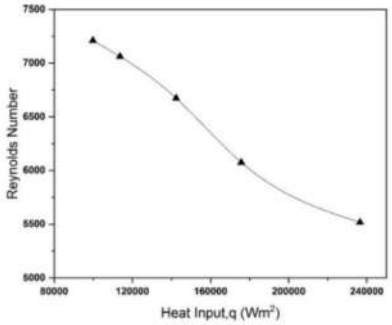

(e) Effect of turbulence on heat flux at VO 1 condition.

Figure 5. Effect of VO1 Condition (full valve opening).

Figure 6 (a-b) shows the temperature variation and the effect of the heat flux. Figure 6 (c-d) indicates the percentage reduction and the index of temperature reduction obtained in the coatings, whereas the temperature reduction achieved due to turbulence effects is observed from figures for 10 µm and 50 µm coated panels.

VO2 Condition (50% of full opening)

In this VO2 opening condition of a foot valve, the discharge and the velocity are 5.85×10^{-3} m^3/s. and 3.5 m/s, respectively. Reynold's number of the flowing air ranges from 4035 to 5784 due to the variation of flowing air temperature and hence the air experiences turbulent formation. The variation in Reynold's number is due to the change in the temperature of the air. Effect of VO2 condition (Partial valve opening) with various responses is shown in Figure 7.

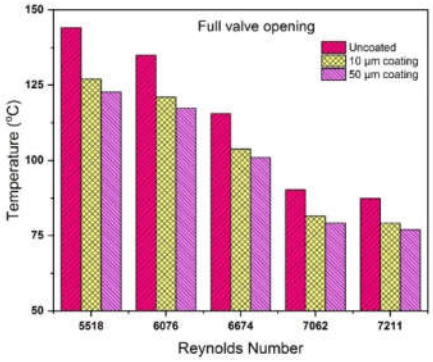

(a) Comparison of temperature with Reynolds number.

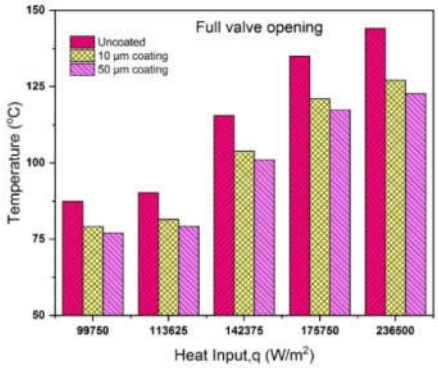

(b) Comparison of heat flux on the coating.

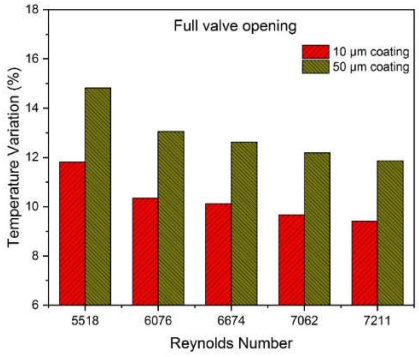

(c) Index of temperature variation with turbulence.

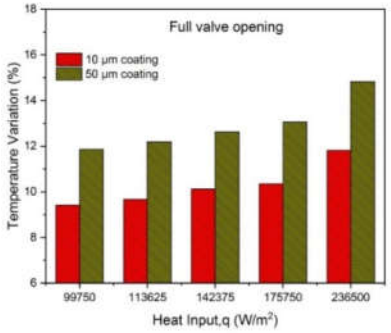

(d) Index of temperature variation with heat flux.

Figure 6. Performance comparison on the coating at VO1 condition.

At 99.75 kW/m^2 heat input, the temperature of the uncoated panel was found to be 95.21 °C, and a temperature of 86.26°C was observed on the 10 µm coated panel and 83.58°C on the 50 µm coated panel. A nearly 9.4% reduction in temperature was calculated in a 10 µm coated panel, while a 12.21% reduction in temperature was noticed in a 50 µm coated panel. The energy input gradually enhanced to a value of 236.5 kW/m^2, the temperature of an uncoated surface plate was found to be 155.92 °C, and a temperature indicator recorded a temperature of 135.37 °C on the 10 µm coated panel and 130.85 °C on the 50 µm coated panel. Nearly 13.18% of the reduction in temperature was noticed in the 10 µm coated panel, and 16.08% of the reduction in temperature was observed in the 50 µm coated panel.

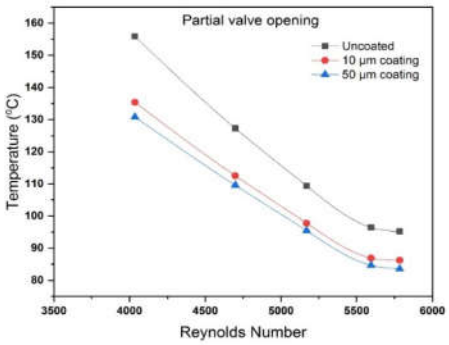

(a) Temperature variation with turbulence temperature.

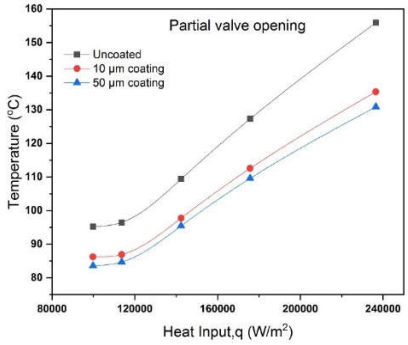

(b) Temperature - heat input.

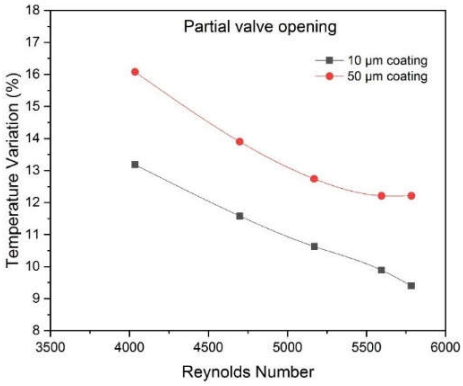

(c) Variation of temperature with Reynolds number.

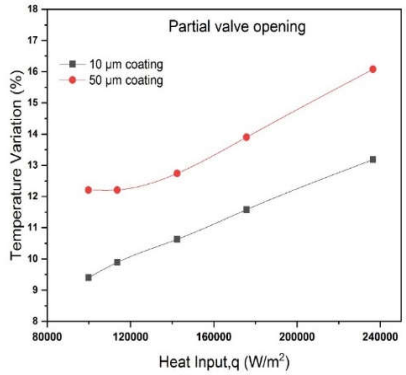

(d) Temperature variations of the coating.

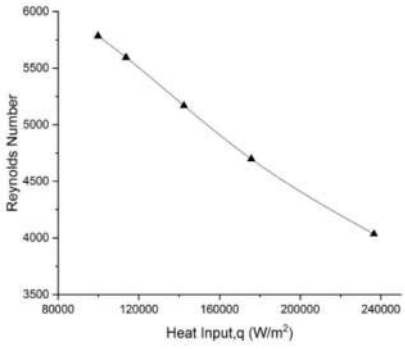

(e) Effect of turbulence on heat flux at VO2 condition.

Figure 7. Effect of VO2 condition (partial valve opening).

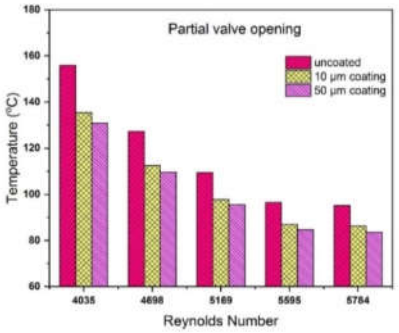

(a) Comparison of temperature with Reynolds number.

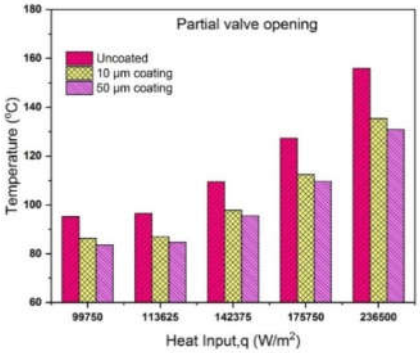

(b) Comparison of heat flux on the coating.

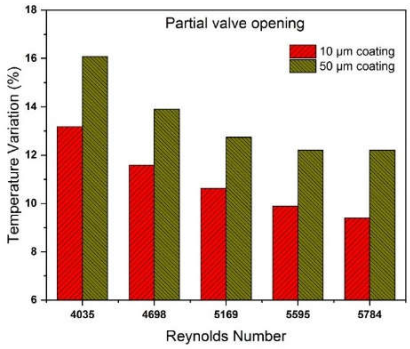

(c) Index of temperature variation with turbulence.

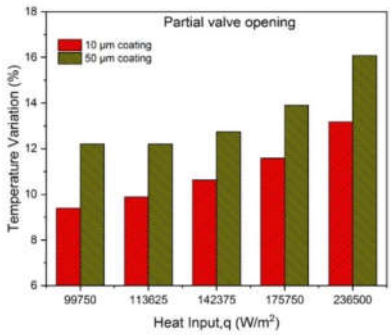

(d) Index of temperature variation with heat flux.

Figure 8. Performance comparison on the coating at VO2 condition (partial valve opening condition).

Figure 8 (a-b) shows the temperature variation and the effect of the heat flux. Figure 8 (c-d) indicates the percentage reduction and the index of temperature reduction obtained in the coatings, whereas the temperature reduction achieved due to turbulence effects is observed from Figures for 10 µm and 50 µm coated panels.

Conductive heat transfer behavior

The figures show the surface temperature attained as a result of various heat loads with an extreme magnitude of 49 kW/m^2 in thicknesses of 10 µm and 50 µm coatings employing aluminium and cast-iron blocks as a source to deliver heat to the system. When aluminium is used as the source material, the surface temperature can reach 300 °C. When cast-iron is used as the source material, a temperature of 600 °C is measured, as can be seen in Figure 9.

The figure shows the variation in temperature and comparison of varying temperatures on coated and uncoated panels for different heat inputs achieved for low-temperature applications (aluminium source blocks) with 10 µm and 50 µm coating thicknesses over a steel substrate, as can be seen in Figure 9.

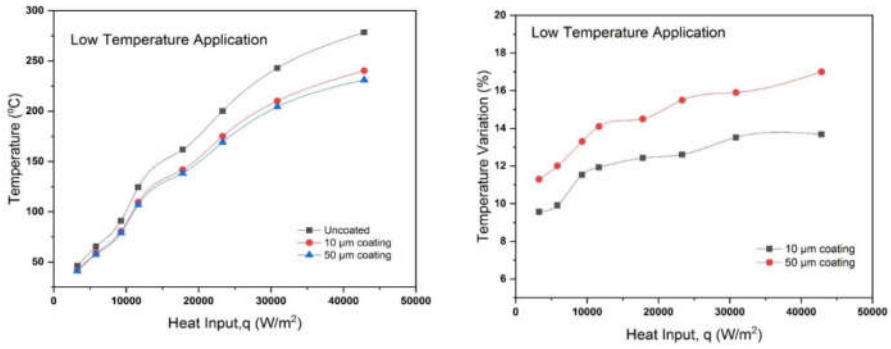

Figure 9. Comparison of temperature and heat input on coated and uncoated panels (aluminium block) and temperature variations of the coated panels (aluminium block).

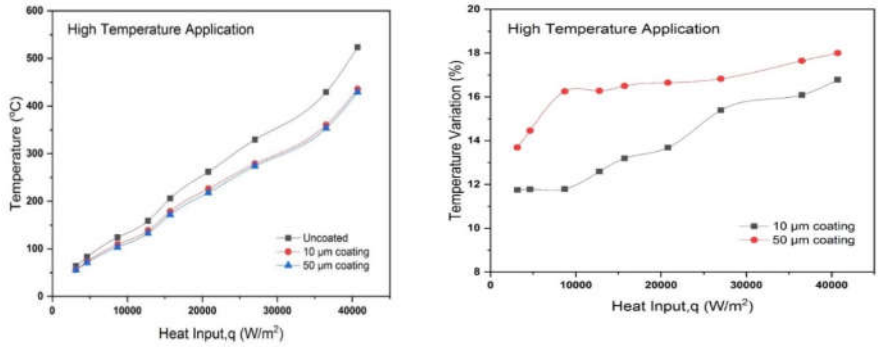

Figure 10. Comparison of temperature and heat input on coated and uncoated panels (CI block) and Temperature variations of the coated panels (CI block).

Figure 10 shows the comparison of temperature and heat input on coated and uncoated panels (CI block) and variation in temperature and comparison of varying temperatures on coated and uncoated panels for different heat inputs achieved for high-temperature applications (cast-iron source blocks) with 10 µm and 50 µm coating thicknesses over a steel substrate. Temperature reductions of 10 to 14% were recorded in coating thicknesses of 10 µm and 14 to 18% in coating thicknesses of 50 µm. The temperature was found to be much lower in the 50 µm thickly coated panel with a nickel-zirconia deposit than in the 10 µm thickly coated panel. This might be due to the increased thermal resistance provided by the thicker coating to the heat flow.

This experimental analysis exhibited the conductive heat transfer characteristics of electro-deposited nickel-zirconia coatings with thicknesses of 10 µm and 50 µm when subjected to a maximum temperature of 600 °C. The encapsulation of nickel ions by nano-zirconia particles resulted in a 14–18% temperature reduction in the 50 µm thickness coating and a 10–14% decrease in temperature in the thickness of 10 µm coated over the mild steel substrate. The temperature was found to be much lower in the 50 µm thickly coated panel with a nickel-zirconia deposit than in the 10 µm thickly coated panel. This might be due to the increased thermal resistance provided by the thicker coating to the heat flow. The convective heat transfer

experiments were focused on exposing the nickel-zirconia coated panels to hot air with different temperatures and various velocities, and it was observed that 10% to 14% of the temperature reduction was achieved in 50 μm thick coated panels, whereas 8% to 11% of the temperature reduction was noticed in 10 μm thick coated panels. From the analysis of variables in convection experiments to achieve the maximum temperature reduction in a 50 μm thick coating by providing a heat input of 197.368 kW/m^2 with a turbulent flow of Re = 4021, the temperatures of the uncoated surface and coated surface were observed as 176.72 °C and 150.28 °C which yields a temperature reduction of 14.96% that is desirable for this study.

CONCLUSION

Nickel-zirconia exhibits a lower wear index 0.056, which is desirable for engineering applications. It has high micro hardness value 740-780 VHN, which indicates that this may replace hard chromium in some cases. The thermal resistance is virtuous in both convection and conduction heat transfer analysis at different temperatures. Hence nickel-zirconia acts as a superior thermal resistive coating over mild steel substrate. This research will clarify how to use nickel-zirconia coating for a specific application.

REFERENCES

1. Kiruthika, P.; Subasri, R.; Jyothirmayi, A.; Sarvani, K.; Hebalkar, N.Y. Effect of plasma surface treatment on mechanical and corrosion protection properties of UV-curable sol-gel based GPTS-ZrO_2 coatings on mild steel. *Surf. Coatings Technol.* **2010**, 204, 1270-1276.
2. Setare, E.; Raeissi, K.; Golozar, M.A.; Fathi, M.H. The structure and corrosion barrier performance of nanocrystalline zirconia electrodeposited coating. *Corros. Sci.* **2009**, 51, 1802-1808.
3. Miranda, J.C.; Ramalho, A. Abrasion resistance of thermal sprayed composite coatings with a nickel alloy matrix and a WC hard phase. Effect of deposition technique and re-melting. *Tribol. Lett.* **2001**, 11, 37-48.
4. Medvedev, V. V.; Mochalov, B. V.; Sazonov, Y. B.; Chernukha, L. G.; Ezhov, I. P. Properties of high-temperature alloys in short-term service conditions. *Met. Sci. Heat Treat.* **1999**, 41, 151.
5. Ghosh, S. Thermal barrier ceramic coatings—A review. *Adv. Ceram. Prog.* **2015**, 111-138.
6. Vaßen, R.; Jarligo, M.O.; Steinke, T.; Mack, D.E.; Stöver, D. Overview on advanced thermal barrier coatings. *Surf. Coat. Technol.* **2010**, 205, 938-942.
7. Poojari, Y.M.; Annigeri, K.S.; Bandekar, N.; Annigeri, K.U.; Patil, A.; Billur, S.; Kottursheṭtar, B.B. An alternative coating material for gas turbine blade for aerospace applications. *J. Phys. Conf. Ser.* **2020**, 1706, 012183.
8. Bapu, G.R.; Jayakrishnan, S. Oxidation characteristics of electrodeposited nickel–zirconia composites at high temperature. *Mater. Chem. Phys.* **2006,** 96, 321-325.
9. Vassen, R.; Stuke, A.; Stöver, D. Recent developments in the field of thermal barrier coatings. *J. Therm. Spray Technol.* **2009**, 18, 181-186.
10. Babu, L.G.; Ramesh, M.; Ravichandran, M.; Mechanical and tribological characteristics of ZrO_2 reinforced Al2014 matrix composites produced via stir casting route. *Mater. Res. Express.* **2019**, 6, 115542.
11. Arghavanian, R.; Parvini Ahmadi, N.; Yazdani, S.; Bostani, B. Fabrication and characterisation of nickel coated Ni-NCZ (nickel coated ZrO_2) composite coating. *Surf. Eng.* **2012**, 28, 503-507.
12. Shongwe, M.B.; Makena, I.M.; Ajibola, O.O.; Olubambi, P.A.; Adams, F.V. Effects of ternary metal additions on corrosion of spark plasma sintered Ni-Fe alloys in H_2SO_4 and NaCl. *Bull. Chem. Soc. Ethiop.* **2018**, 32, 337-349.
13. Fayomi, O.S.I.; Popoola, A.P.I.; Monyai, T. Improving the properties of mild steel by ternary multilayer composite coating via electrodeposition route. *Bull. Chem. Soc. Ethiop.* **2016**, 30, 449-456.